

High upper critical field and irreversibility field in MgB₂ coated-conductor fibers

V. Ferrando,^{a)} P. Orgiani,^{b)} A. V. Pogrebnyakov, J. Chen, Qi Li,
J. M. Redwing, and X. X. Xi^{c)}

Materials Research Institute, The Pennsylvania State University, University Park, Pennsylvania 16802

J. E. Giencke and Chang-Beom Eom

*Department of Materials Science and Engineering and Applied Superconductivity Center,
University of Wisconsin, Madison, Wisconsin 53706*

Qing-Rong Feng

*Department of Physics and State Key Laboratory for Mesoscopic Physics, Peking University,
Beijing 100871, People's Republic of China*

J. B. Betts and C. H. Mielke

*National High Magnetic Field Laboratory, Los Alamos National Laboratory, Los Alamos,
New Mexico 87545*

(Received 7 September 2005; accepted 14 November 2005; published online 14 December 2005)

We report on structural and superconducting properties of round MgB₂ coated-conductor fibers deposited by hybrid physical-chemical vapor deposition on SiC fibers. The coating is polycrystalline and composed of elongated crystallites with dimensions less than 1 μm in length and 0.2 μm in width. The pure MgB₂ fiber shows a zero-resistance T_c of 39.3 K. The carbon-alloyed fibers show a high upper critical field of 55 T at 1.5 K and a high irreversibility field of 40 T at 1.5 K. The result demonstrates great potential of MgB₂ coated conductors for superconducting magnets. © 2005 American Institute of Physics. [DOI: 10.1063/1.2149289]

The recently discovered superconductor MgB₂ (see Ref. 1) is a promising material for high-magnetic-field applications.² The transition temperature at 40 K allows practical operation above 20 K using cryocoolers. Unlike high temperature superconductors where critical current density J_c drops sharply across the grain boundary when the grains are misaligned, grain boundaries do not degrade J_c in MgB₂.^{3,4} Wires and tapes of MgB₂ have been made using the so-called “powder-in-tube” (PIT) technique with encouraging results.^{5–7} MgB₂ conductors also promise lower cost.³ Recently, we have shown record high values of upper critical field $H_{c2}(0)$ over 60 T in textured carbon-alloyed MgB₂ thin films produced by hybrid physical-chemical vapor deposition (HPCVD).⁸ Whether such record high values can be achieved in forms more suitable for practical conductors is of great interest. Here we report on polycrystalline carbon-alloyed MgB₂ coated-conductor fibers with high H_{c2} (the field at which a superconductor becomes normal) and high irreversibility field H_{irr} (the field at which a superconductor ceases to carry supercurrent). The result demonstrates great potential of the coated conductor approach towards MgB₂ high-field wires for superconducting magnets.

Coated conductors have been widely studied for high temperature superconductors.^{3,4} Coated conductors have also been explored for MgB₂ by sputtering on Hastelloy⁹ and by electroplating on stainless steel.¹⁰ These works have generated H_{c2} and H_{irr} values similar to those of PIT MgB₂ wires. In this work, the MgB₂ coated conductors were grown by HPCVD¹¹ on round SiC fibers with a tungsten core.^{12,13} De-

tails of the HPCVD process have been described elsewhere.¹¹ The SiC/W fibers, about 1 cm in length, were placed on the top horizontal surface of the susceptor (heater) and heated to 685–720 °C in H₂ carrier gas during the deposition. Heated Mg chips placed near the SiC fibers served as the Mg source while B₂H₆ was the B source. The deposition rate was about 0.1 $\mu\text{m}/\text{min}$ at 700 °C. Some fibers were coated multiple times to achieve thicker coating. For the deposition of the carbon-alloyed MgB₂ coating, we added bis(methylcyclopentadienyl)magnesium [(MeCp)₂Mg], a carbon-containing metalorganic magnesium precursor, to the gas flow during the deposition, and the carbon content in the coating was controlled by the flow rate of a secondary hydrogen flow passing through the (MeCp)₂Mg bubbler.¹⁴

Figure 1 shows scanning electron microscope (SEM) images of a round MgB₂ coated-conductor fiber. The diameter of the SiC fiber is $\sim 100 \mu\text{m}$ with a tungsten core of $\sim 10 \mu\text{m}$.¹³ Except for a defect spot, Fig. 1(a) shows a uniform coating of the fiber. Figure 1(b) shows that the SiC fiber has a columnar structure along the radial direction.¹² The MgB₂ coating, seen as the bright layer on the surface of the fiber, is about 0.75 μm in thickness. Although the fiber was coated only once, it shows a relatively uniform thickness of the MgB₂ layer without shadow effect, which is due to the high gas pressure (100 Torr) and the diffusive nature of the deposition process. Figure 1(c) is a blown-up view that shows more clearly the microstructure of the coating. The MgB₂ coating has a granular structure with randomly oriented crystallites. The grains are elongated with length less than 1 μm and width of 0.2 μm . This microstructure is very similar to those in some early polycrystalline MgB₂ films.¹⁵

The structure of the MgB₂ coating was further studied by x-ray diffraction using a two-dimensional area detector. The integrated area diffraction θ – 2θ scan is shown in Fig. 2. The peaks from the SiC fiber, marked by “*,” indicate that SiC is

^{a)}On leave from University of Genoa/INFM-LAMIA, Genoa 16146, Italy.

^{b)}On leave from University of Naples/INFM-Coherentia, Naples I-80125, Italy.

^{c)}Author to whom correspondence should be addressed; electronic mail: xxx4@psu.edu

Report Documentation Page			Form Approved OMB No. 0704-0188		
Public reporting burden for the collection of information is estimated to average 1 hour per response, including the time for reviewing instructions, searching existing data sources, gathering and maintaining the data needed, and completing and reviewing the collection of information. Send comments regarding this burden estimate or any other aspect of this collection of information, including suggestions for reducing this burden, to Washington Headquarters Services, Directorate for Information Operations and Reports, 1215 Jefferson Davis Highway, Suite 1204, Arlington VA 22202-4302. Respondents should be aware that notwithstanding any other provision of law, no person shall be subject to a penalty for failing to comply with a collection of information if it does not display a currently valid OMB control number.					
1. REPORT DATE 14 DEC 2005		2. REPORT TYPE		3. DATES COVERED 00-00-2005 to 00-00-2005	
4. TITLE AND SUBTITLE High upper critical field and irreversibility field in MgB2 coated-conductor fibers			5a. CONTRACT NUMBER		
			5b. GRANT NUMBER		
			5c. PROGRAM ELEMENT NUMBER		
6. AUTHOR(S)			5d. PROJECT NUMBER		
			5e. TASK NUMBER		
			5f. WORK UNIT NUMBER		
7. PERFORMING ORGANIZATION NAME(S) AND ADDRESS(ES) University of Wisconsin-Madison, Department of Materials Science and Engineering, Madison, WI, 53706			8. PERFORMING ORGANIZATION REPORT NUMBER		
9. SPONSORING/MONITORING AGENCY NAME(S) AND ADDRESS(ES)			10. SPONSOR/MONITOR'S ACRONYM(S)		
			11. SPONSOR/MONITOR'S REPORT NUMBER(S)		
12. DISTRIBUTION/AVAILABILITY STATEMENT Approved for public release; distribution unlimited					
13. SUPPLEMENTARY NOTES					
14. ABSTRACT					
15. SUBJECT TERMS					
16. SECURITY CLASSIFICATION OF:			17. LIMITATION OF ABSTRACT Same as Report (SAR)	18. NUMBER OF PAGES 3	19a. NAME OF RESPONSIBLE PERSON
a. REPORT unclassified	b. ABSTRACT unclassified	c. THIS PAGE unclassified			

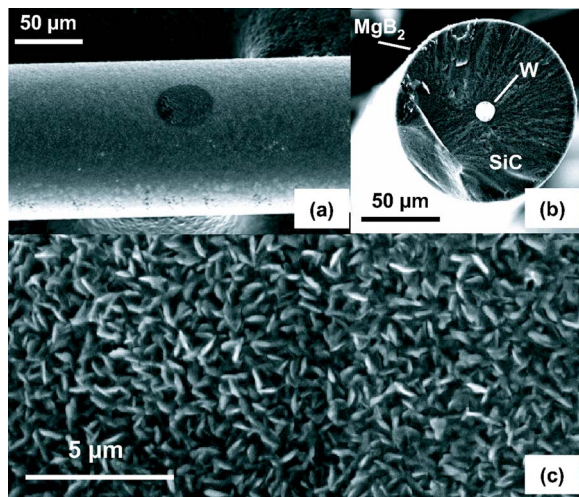


FIG. 1. (a) Scanning electron microscope (SEM) images of a MgB_2 coated-conductor fiber. (b) A cross-section image of the MgB_2 coated-conductor fiber. (c) A blown-up SEM image of the surface, showing elongated MgB_2 crystallites with random orientations.

of the 3C polytype (β -SiC, zinc blende structure).¹⁶ Several diffraction peaks off different MgB_2 planes are seen, indicating that the MgB_2 crystallites are oriented randomly. The polycrystalline nature of the microstructure and the small grain size make the diffraction intensity from MgB_2 weak. The lattice constants of the MgB_2 layer are $a = 3.078 \pm 0.01$ Å and $c = 3.514 \pm 0.005$ Å, matching very well with the bulk values of pure MgB_2 .¹ Also observed are diffraction peaks due to Mg_2Si . It could be the result of reaction of Mg with SiC¹⁷ or with the free Si existing in the SiC fiber.¹³

The superconducting properties of the coated-conductor fibers are similar to those in epitaxial pure MgB_2 and textured carbon-alloyed MgB_2 films deposited by HPCVD. For example, a pure MgB_2 fiber shows a zero-resistance transition temperature T_c of 39.3 K. It has a residual resistivity of $\rho_0 \sim 30$ $\mu\Omega$ cm, much higher than that in the clean epitaxial HPCVD MgB_2 films ($\rho_0 \sim 0.28$ $\mu\Omega$ cm¹⁸), and a residual resistance ratio of $RRR = R(300 \text{ K})/R(50 \text{ K}) = 2.54$, much smaller than that in the clean films ($RRR \sim 30$ ¹⁸). This is due to the granular nature of the layer and the existence of semi-conducting Mg_2Si , presumably at the grain boundaries.

Measurements in magnetic field were carried out at the National High Magnetic Field Laboratory at Florida State

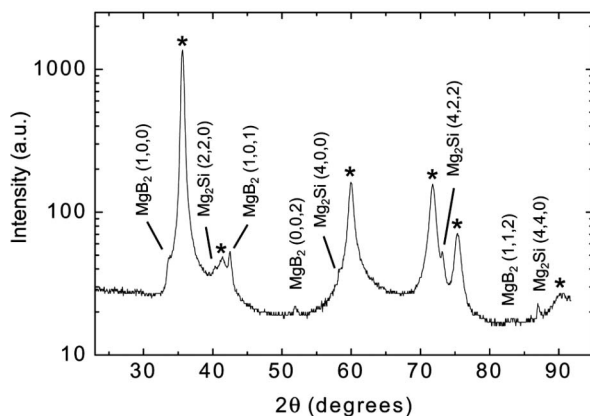


FIG. 2. Integrated x-ray diffraction θ - 2θ scan of a pure MgB_2 coated-conductor fiber collected using a two-dimensional area detector.

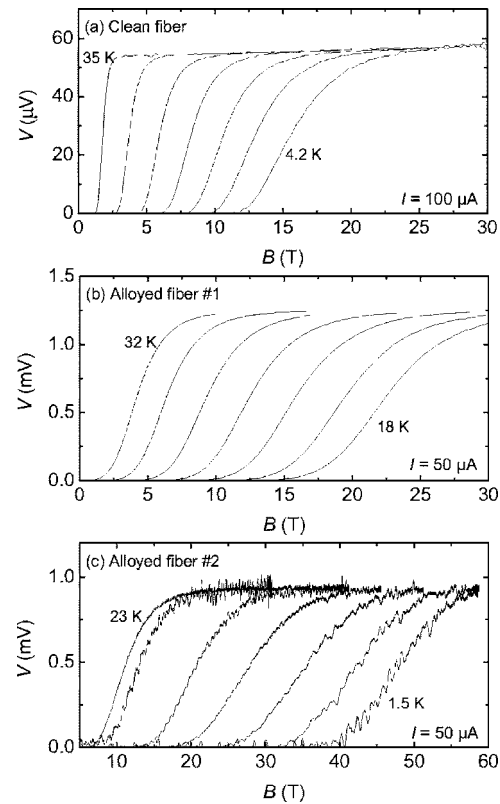


FIG. 3. Voltage-magnetic field curves for (a) a pure MgB_2 fiber, (b) carbon-alloyed MgB_2 fibers 1, and (c) carbon-alloyed MgB_2 fibers 2. For each set of data, the lowest and the highest temperatures of the measurements are shown.

University (dc field, up to 30 T) and Los Alamos National Laboratory (pulsed field, up to 60 T). Figure 3 shows voltage versus applied magnetic field curves measured at different temperatures for three MgB_2 coated-conductor fibers: (a) a pure clean MgB_2 fiber, (b) carbon-alloyed MgB_2 fiber 1, and (c) carbon-alloyed MgB_2 fiber 2. The measurement currents are 100, 50, and 50 μA for the three fibers, respectively. Carbon alloying suppresses T_c and increases resistivity of the coating, leading to larger voltage signals in the carbon-alloyed MgB_2 fibers than in the pure MgB_2 fiber. From these curves, H_{c2} and H_{irr} are determined by the following criteria: $R(H_{c2}) = 0.9R_0$ and $R(H_{irr}) = 0.1R_0$, where R_0 is the residual resistance above the superconducting transition.

Previously, we have shown textured films of carbon-alloyed MgB_2 prepared by HPCVD H_{c2} of 51 T in parallel field and 35 T in perpendicular field at 4.2 K.⁸ Since the MgB_2 grains in the coated-conductor layers are randomly oriented, MgB_2 grains with a - b grains parallel to the applied field become normal at a higher field than those whose a - b grains are perpendicular to the applied field, with grains of other orientations in between. Because H_{c2} measures the onset of superconductivity, the measured H_{c2} values in the coated-conductor fibers should be similar to the higher, parallel-field H_{c2} in the textured films. On the other hand, as soon as the superconducting MgB_2 grains form a continuous path, the fiber will reach zero resistance, which is measured by the H_{irr} values in the coated-conductor fibers.

Figure 4 shows the temperature dependencies of (a) H_{c2} and (b) H_{irr} for the three fibers in Fig. 3. The clean fiber has an $H_{c2}(4.2 \text{ K})$ of 20 T, which is dramatically enhanced by carbon alloying. At $T = 1.5 \text{ K}$, alloyed fiber 2 shows an H_{c2} of

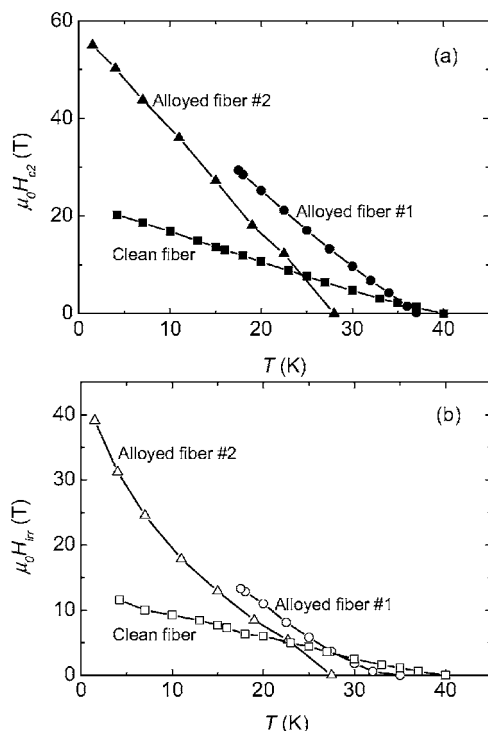


FIG. 4. Temperature dependencies of (a) H_{c2} and (b) H_{irr} for the three MgB_2 coated-conductor fibers shown in Fig. 3.

55 T, and at $T=25$ K, alloyed fiber 1 has an H_{c2} of 17 T. The enhancement of H_{c2} by carbon alloying can be qualitatively explained by the modifications of intraband and interband scattering in the two (σ and π) bands of MgB_2 .¹⁹ Similar dramatic enhancement by carbon alloying is also seen in H_{irr} , indicating an increase in the flux pinning by carbon alloying. An H_{irr} value of 40 T at $T=1.5$ K is obtained in alloyed fiber 2, while H_{irr} is 5.8 T at $T=25$ K for alloyed fiber 1. The H_{c2} and H_{irr} reported here are substantially higher than those previously reported for PIT MgB_2 wires ($H_{c2} \sim 37$ T in carbon-doped MgB_2 PIT wires²⁰ and $H_{irr} \sim 25.4$ T at 4.2 K in MgB_2 PIT wires with addition of SiC nanoparticles²¹). The differences may be due to the different microstructures: in carbon-doped bulk MgB_2 , the a axis shrinks but c axis remains constant with increasing carbon concentrations,²² whereas in HPCVD films both a and c axes expand with carbon alloying.¹⁴

The result here demonstrates that epitaxy and texture are not necessary for achieving high H_{c2} and H_{irr} . This is important for practical manufacturing of MgB_2 conductor wires. The high H_{c2} and H_{irr} are very attractive for superconducting magnets in magnetic resonance imaging (MRI) systems.²³ In particular, the operating temperature above 20 K allows replacement of liquid helium by efficient cryocoolers, so that MRI systems could become lighter, of lower operation cost, more reliable, and more accessible to populations in remote locations or in developing countries.^{24,25} The HPCVD technique used here is adaptable to scale up for continuous and uniform coating of long length fibers. High MgB_2 deposition rate, which is important for manufacturing, has been demonstrated up to 1.2 $\mu\text{m}/\text{min}$ by HPCVD.²⁶ Although the large diameter SiC fiber used in this work is not the desirable substrate for practical conductor wires because it is brittle and costly, MgB_2 coatings can be made on inexpensive and strong metallic wires such as stainless steel.^{10,26} Therefore,

the MgB_2 coated conductor fabricated using HPCVD could be seriously considered as a potential alternative to the current Nb-based high-field conductors.

This work is supported in part by the NSF under Grant Nos. DMR-0405502 (Q.L.), DMR-0306746 (X.X.X. and J.M.R.), and the MRSEC for Nanostructure Materials at University of Wisconsin (C.B.E.), and by ONR under Grant Nos. N00014-00-1-0294 (X.X.X.) and N0014-01-1-0006 (J.M.R.). Experiments performed at NHMFL were supported by NSF, the State of Florida and the U.S. Department of Energy.

- ¹J. Nagamatsu, N. Nakagawa, T. Muraoka, Y. Zenitani, and J. Akimitsu, *Nature* (London) **410**, 63 (2001).
- ²D. C. Larbalestier, L. D. Cooley, M. O. Rikel, A. A. Polyanskii, J. Jiang, S. Patnaik, X. Y. Cai, D. M. Feldmann, A. Gurevich, A. A. Squitieri, M. T. Naus, C. B. Eom, E. E. Hellstrom, R. J. Cava, K. A. Regan, N. Rogado, M. A. Hayward, T. He, J. S. Slusky, P. Khalifah, K. Inumaru, and M. Haas, *Nature* (London) **410**, 186 (2001).
- ³R. M. Scanlan, A. P. Malozemoff, and D. C. Larbalestier, *Proc. IEEE* **92**, 1639 (2004).
- ⁴D. C. Larbalestier, A. Gurevich, D. M. Feldmann, and A. A. Polyanskii, *Nature* (London) **414**, 368 (2001).
- ⁵S. Jin, H. Mavoori, C. Bower, and R. B. van Dover, *Nature* (London) **411**, 563 (2001).
- ⁶G. Grasso, A. Malagoli, C. Ferdeghini, S. Roncallo, V. Braccini, A. S. Siri, and M. R. Cimberle, *Appl. Phys. Lett.* **79**, 230 (2001).
- ⁷R. Flükiger, H. L. Suo, N. Musolino, C. Beneduce, P. Toulemonde, and P. Lezza, *Physica C* **385**, 286 (2003).
- ⁸V. Braccini, A. Gurevich, J. Giencke, M. Jewell, C. Eom, D. Larbalestier, A. Pogrebnikov, Y. Cui, B. T. Liu, Y. F. Hu, J. M. Redwing, Q. Li, X. X. Xi, R. Singh, R. Gandikota, J. Kim, B. Wilkens, N. Newmann, J. Rowell, B. Moeckly, V. Ferrando, C. Tarantini, D. Marr, M. Putti, C. Ferdeghini, R. Vaglio, and E. Haanappel, *Phys. Rev. B* **71**, 012504 (2005).
- ⁹K. Komori, K. Kawagishi, Y. Takano, H. Fujii, S. Arisawa, H. Kumakura, M. Fukutomi, and K. Togano, *Appl. Phys. Lett.* **81**, 1047 (2002).
- ¹⁰H. Abe, K. Nishida, M. Imai, H. Kitazawa, and K. Yoshii, *Appl. Phys. Lett.* **85**, 6197 (2004).
- ¹¹X. H. Zeng, A. V. Pogrebnikov, A. Kotcharov, J. E. Jones, X. X. Xi, E. M. Lysczek, J. M. Redwing, S. Y. Xu, Q. Li, J. Lettieri, D. G. Schlom, W. Tian, X. Q. Pan, and Z. K. Liu, *Nat. Mater.* **1**, 35 (2002).
- ¹²R. J. Suplinskas and J. V. Marzik, in *Handbook of Reinforcements for Plastics*, edited by J. V. Milewski and H. S. Katz (Van Nostrand Reinhold, New York, 1987), pp. 340–363.
- ¹³Y. Le Petitcorps, M. Lahaye, R. Paillet, and R. Naslain, *Compos. Sci. Technol.* **32**, 31 (1988).
- ¹⁴A. V. Pogrebnikov, X. X. Xi, J. M. Redwing, V. Vaithyanathan, D. G. Schlom, A. Soukiasian, S. B. Mi, C. L. Jia, J. Giencke, C. B. Eom, J. Chen, Y. F. Hu, Y. Cui, and Q. Li, *Appl. Phys. Lett.* **85**, 2017 (2004).
- ¹⁵M. Paranthaman, C. Cantoni, H. Y. Zhai, H. M. Christen, T. Aytug, S. Sathyanarayana, E. D. Specht, J. R. Thompson, D. H. Lowndes, H. R. Kerchner, and D. K. Christen, *Appl. Phys. Lett.* **78**, 3669 (2001).
- ¹⁶U. Rössler and D. Strauch, in *LANDOLT-BÖRNSTEIN: Numerical Data and Functional Relationships in Science and Technology*, New Series, Vol. III/41A1 α , edited by U. Rössler (Springer, Berlin, 2001), pp. 261–322.
- ¹⁷S. X. Dou, V. Braccini, S. Soltanian, R. Klie, Y. Zhu, S. Li, X. L. Wang, and D. Larbalestier, *J. Appl. Phys.* **96**, 7549 (2004).
- ¹⁸A. V. Pogrebnikov, J. M. Redwing, J. E. Jones, X. X. Xi, S. Y. Xu, Q. Li, V. Vaithyanathan, and D. G. Schlom, *Appl. Phys. Lett.* **82**, 4319 (2003).
- ¹⁹A. Gurevich, *Phys. Rev. B* **67**, 184515 (2003).
- ²⁰R. H. T. Wilke, S. L. Budko, P. C. Canfield, D. K. Finnemore, and S. T. Hannahs, *cond-mat/0507151* (2005).
- ²¹M. D. Sumption, M. Bhatia, M. Rindfleisch, M. Tomsic, S. Soltanian, S. X. Dou, and E. W. Collings, *Appl. Phys. Lett.* **86**, 092507 (2005).
- ²²S. Lee, T. Masui, A. Yamamoto, H. Uchiyama, and S. Tajima, *Physica C* **397**, 7 (2003).
- ²³G. Morrow, *IEEE Trans. Appl. Supercond.* **10**, 744 (2000).
- ²⁴E. T. Laskaris, U.S. Patent No. 4,924,198 (8 May 1990).
- ²⁵B. X. Xu, S. Schnurer, K. Obasli, M. Mruzek, O. Ige, R. Lochner, J. Helbing, and D. Mantone, *IEEE Trans. Magn.* **32**, 2637 (1996).
- ²⁶C. P. Chen, Q. R. Feng, Z. Z. Gan, G. C. Xiong, J. Xu, Y. F. Liu, L. W. Kong, L. Li, Z. Jia, J. P. Guo, C. G. Zhuang, L. L. Ding, L. P. Chen, F. Li, and K. C. Zhang, *Chin. Sci. Bull.* **50**, 719 (2005).